

Electric-dipole-active magnetic resonance in the conical-spin magnet $\text{Ba}_2\text{Mg}_2\text{Fe}_{12}\text{O}_{22}$

N. Kida,¹ D. Okuyama,² S. Ishiwata,² Y. Taguchi,² R. Shimano,^{1,3} K. Iwasa,⁴ T. Arima,⁵ and Y. Tokura^{1,2,6}

¹Multiferroics Project (MF), ERATO, Japan Science and Technology Agency (JST), c/o Department of Applied Physics, The University of Tokyo, Tokyo 113-8656, Japan

²Cross-Correlated Materials Research Group (CMRG), ASI, RIKEN, Wako 351-0198, Japan

³Department of Physics, The University of Tokyo, Tokyo 113-0033, Japan

⁴Department of Physics, Tohoku University, Sendai 980-8578, Japan

⁵Institute of Multidisciplinary Research for Advanced Materials, Tohoku University, Sendai 980-8577, Japan

⁶Department of Applied Physics, The University of Tokyo, Tokyo 113-8656, Japan

(Received 27 October 2009; published 10 December 2009)

Electric-field (E) drive of magnetic resonance in a solid has been a big challenge in condensed-matter physics and emerging spintronics. We demonstrate the appearance of distinct magnetic excitations driven by the light E component in a hexaferrite $\text{Ba}_2\text{Mg}_2\text{Fe}_{12}\text{O}_{22}$. In the conical-spin state even with no spontaneous electric polarization (P_s), a sharp and intense resonance is observed around 2.8 meV for the light E vector parallel to the magnetic propagation vector in accord with the inelastic neutron scattering spectrum at the magnetic zone center. As the generic characteristic of the conical state, a weak magnetic field (~ 2 kOe) can modify the spin structure, leading to a remarkable change (terahertz magnetochromism) in spectral shape and intensity (by $\sim 200\%$) of the electric-dipole-active magnetic resonance. The present observation implies that potentially many magnets with noncollinearly ordered spins may host such an electric-dipole-active resonance, irrespective of the presence or absence of P_s .

DOI: [10.1103/PhysRevB.80.220406](https://doi.org/10.1103/PhysRevB.80.220406)

PACS number(s): 75.80.+q, 76.50.+g, 75.40.Gb

In general, magnetization dynamics in a solid as carried by the collective precession of constituent spins shows the resonance with oscillating magnetic field at gigahertz to terahertz frequencies, known as magnetic resonance.¹ Contrary to this conventional mechanism, the electric-field (E) drive of this magnetic resonance, although predicted long time ago,² is highly nontrivial but the most demanding function in the future spin electronics.^{3,4} The possible signature of such an electric-dipole-active resonance excitation, frequently termed electromagnon, was recently observed in compounds with both magnetic and ferroelectric orders (multiferroics^{5,6}), such as the spiral-spin-order-induced multiferroics TbMnO_3 at terahertz frequencies.⁷ At an early stage of the study, the origin of the electromagnon was considered to result from either the electric activity induced by the antisymmetric (Dzyaloshinskii-Moriya) interaction or the E modulation of the spiral-spin plane defined by neighboring spins ($S_i \times S_j$).^{8,9} However, more recent spectroscopic studies on light-polarization and magnetic-field dependences for DyMnO_3 clearly negated a possibility of this mechanism.¹⁰ Rather, the symmetric exchange mechanism ($S_i \cdot S_j$) as a result of the magnetic modulation of the local electric dipoles was proposed in terms of the underlying ionic lattice symmetry¹¹ or orbital ordering structure.¹² In contrast to the electromagnons in multiferroics with antiferromagnetic order, as previously discussed for perovskite RMnO_3 (R represents rare-earth ions),⁷⁻¹⁴ hexagonal YMnO_3 ,¹⁵ BiFeO_3 ,^{16,17} and RMn_2O_5 ,^{18,19} a gigantic response to external static magnetic field—i.e., a dramatic change in the spectral shape and intensity of the electromagnons—is expected for ferromagnetic compounds.

Here, we show the finding of the sharp and intense electric-dipole-active magnetic resonance in a Y -type hexaferrite, $\text{Ba}_2\text{Mg}_2\text{Fe}_{12}\text{O}_{22}$, with conical (i.e., ferromagnetic plus spiral) spin order. The resonance observed around 2.8 meV (0.7 THz) is strongly polarized for the light E vector along

the magnetic propagation vector k ($\parallel[001]$) in the conical-spin state below 50 K, irrespective of the presence or absence of the spontaneous electric polarization. We also reveal the magnon branch with parabolic dispersion and the corresponding gap energy (2.8 meV). Reflecting the ferromagnetic nature of the compound, such a conical-spin state is modified to a large extent by a relatively weak magnetic field (e.g., ~ 2 kOe), leading to a remarkable change in intensity (by $\sim 200\%$) and shape of the electric-dipole-active magnetic resonance. This strongly magnetochromic resonance is contrastive to the electromagnon spectra of conventional multiferroics with antiferromagnetic nature,^{7,9,10,13-19} in which the application of magnetic field up to the tesla order can hardly alter the excitation spectra.

Among magnetoelectric materials found so far, the Y -type hexagonal ferrite $\text{Ba}_2\text{Mg}_2\text{Fe}_{12}\text{O}_{22}$ investigated here is a rare example with respect to the high sensitivity to external magnetic field H , as demonstrated by the low- H (~ 100 Oe) generation and control of the ferroelectric polarization P_s .^{20,21} This results from the ferrimagnetic nature of $\text{Ba}_2\text{Mg}_2\text{Fe}_{12}\text{O}_{22}$, whose large magnetic moments are aligned by a low H on the order of 100 Oe,²² in contrast with the other multiferroics.²³⁻²⁵ $\text{Ba}_2\text{Mg}_2\text{Fe}_{12}\text{O}_{22}$ consists of two magnetic sublattice blocks, L and S blocks, stacking alternately along $[001]$ [see Fig. 1(d)], which bear, respectively, the opposite large and small magnetization M , causing the ferrimagnetism even at high temperatures exceeding room temperature.²² Below 195 K, the proper screw spin structure is developed with k along $[001]$ with a turn angle φ between the adjacent L spins,²⁶ while the magnetic easy axis still lies in the in plane; φ reaches the maximum about 75° at around 60 K on cooling.²⁶ With further decreasing temperature T below 50 K, the longitudinal conical-spin structure [Fig. 1(d)] evolves with the cone axis parallel to k .²⁰ Furthermore, the transverse conical-spin structure with the cone axis perpendicular to k is realized by the declining of the spin cone

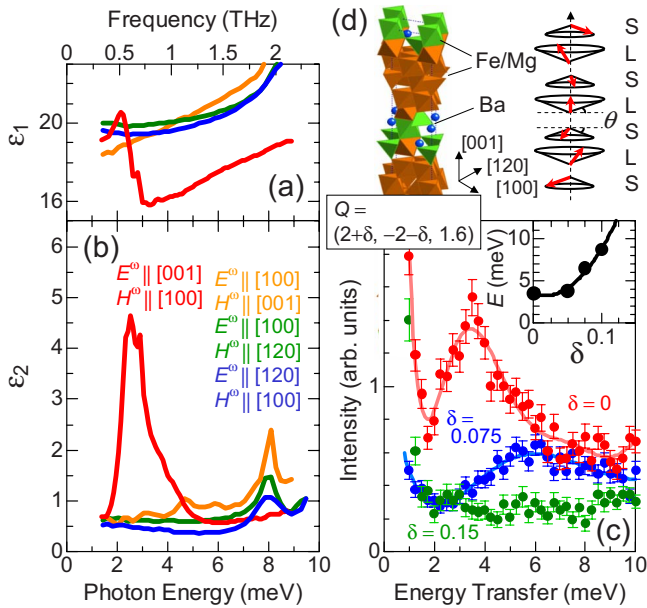


FIG. 1. (Color online) Electric-dipole-active magnetic resonance in $\text{Ba}_2\text{Mg}_2\text{Fe}_{12}\text{O}_{22}$, as revealed by the combined studies of terahertz time-domain spectroscopy and inelastic neutron scattering. (a) Real ϵ_1 and (b) imaginary ϵ_2 parts of the complex dielectric constant spectra $\epsilon(\omega)$, measured at 5 K in the ordered conical-spin phase in zero magnetic field. The crystallographic axes with respect to E^ω and H^ω are indicated in (b). (c) Inelastic neutron scattering spectra (closed circles) near the magnetic zone center $Q=(2, -2, 1.6)$, measured at 10 K. The solid lines are merely the guide to the eyes. Inset shows the magnon dispersion curve along the in-plane direction. The solid line is a least-squares fit by assuming the δ^2 dependence. (d) Schematic illustrations of the hexagonal crystal structure and the conical-spin structure with crystal orientations. The conical angle θ is as defined in (d).

toward the direction of the external H on the order of 100 Oe, producing P_s (Ref. 27) along the direction perpendicular to k and H .²⁰ These unique characteristics of $\text{Ba}_2\text{Mg}_2\text{Fe}_{12}\text{O}_{22}$, in which the spin structure can be easily modified by T and H , provide an interesting arena to test a generic electric-dipole-active magnetic resonance and its dramatic H control.

The terahertz time-domain spectroscopy in a transmission geometry was performed to directly determine the complex optical constants $n = \sqrt{\epsilon\mu}$, where ϵ and μ are the complex dielectric constant and the magnetic permeability, respectively. The direction of the light polarization was carefully set parallel to the respective crystallographic axes [i.e., [001] (out of plane); [100] and [120] (both are orthogonal in the in plane)] of the hexagonal structure [Fig. 1(d)] by a wire-grid polarizer. Based on the detailed light-polarization dependence using two crystal plates with different orientations [Fig. 1(b)], we confirmed that the contribution of $\mu(\omega)$ to $n(\omega)$ is negligible [i.e., $\mu(\omega) \approx 1$]. Thus, the quantity of $\epsilon(\omega)$ is used in this Rapid Communication. The details of our experimental setup and the analytical procedure are described in Ref. 10. For measurements in H supplied by the electromagnet (up to 2 kOe), we adopted the Voigt geometry to exclude the contributions of the magneto-optical effect like the Faraday rotation. The single crystals were prepared

by a flux method²⁰ and characterized by x-ray diffraction, magnetization, and pyroelectric measurements, the results of which were all consistent with a previous report.²⁰

There is a noticeable optical anisotropy in the terahertz (meV range of photon energy; 1 THz \approx 4 meV) spectra for the ordered conical-spin phase. Figures 1(a) and 1(b) show the real (ϵ_1) and imaginary (ϵ_2) parts of $\epsilon(\omega)$ of $\text{Ba}_2\text{Mg}_2\text{Fe}_{12}\text{O}_{22}$ at 5 K with four polarization configurations, respectively. The most notable feature is the appearance of a gigantic sharp resonance around 2.8 meV (0.7 THz), clearly seen as a peak structure in $\epsilon_2(\omega)$ [Fig. 1(b)] and a dispersive structure in $\epsilon_1(\omega)$ [Fig. 1(a)], when electric-field E^ω and magnetic-field H^ω polarizations of light were set parallel to [001] and [100], respectively. This sharp resonance can be attributed to an electric-dipole-active mode with E^ω along [001]; the measurement, in which the direction of E^ω was rotated from [001] to [120] while keeping the direction of H^ω (\parallel [100]) unchanged ($E^\omega \parallel$ [120] and $H^\omega \parallel$ [100]) showed no signature of the resonance in $\epsilon(\omega)$ at this frequency. In the latter configuration, however, another resonance can be discerned around 8 meV (2 THz), while the magnitude of ϵ_2 is smaller than that of 2.8 meV peak for $E^\omega \parallel$ [001] by a factor of ~ 5 . This mode is persistently observed irrespective of the rotation of the direction of E^ω within the in plane ([100] and [120]), whereas it disappears for $E^\omega \parallel$ [001]. Therefore, this mode can be assigned also to an electric-dipole-active mode, while allowed only for the in-plane E^ω . We observed the negligible effect of H on this mode (not shown). In the following, we focus on the nature of the lower-lying electric-dipole-active mode around 2.8 meV polarized along [001].

To clarify its origin, we measured the inelastic neutron scattering spectra as well, using a triple-axis spectrometer TOPAN installed at JRR-3 research reactor in Japan Atomic Energy Agency (JAEA), where the scattering neutron energy was set at 13.5 meV. Figure 1(c) presents the magnetic excitation spectra near the magnetic zone center $Q=(2+\delta, -2-\delta, 1.6)$ in the Brillouin zone, measured at 10 K. At the magnetic zone center ($\delta=0$), we clearly observe the pronounced magnetic excitation peaking around 3 meV. Although the spectral shape is rather broad compared to $\epsilon_2(\omega)$ [Fig. 1(b)] due to the resolution function extending over the Brillouin zone, the observed peak position nearly coincides with that of $\epsilon_2(\omega)$. The peak position shifts to the higher energy with increasing the in-plane Q vector, as exemplified by the spectrum at $\delta=0.075$. Finally, the peak structure diminishes in the measured energy range when δ exceeds 0.15. The measured magnon dispersion relation along the in-plane direction of $\text{Ba}_2\text{Mg}_2\text{Fe}_{12}\text{O}_{22}$ is parabolic with respect to δ [inset of Fig. 1(c)], being similar to the magnon dispersion curve close to the band minimum of rare-earth-metal magnets with a helical structure.²⁸ Based on the complementary measurements of the magnon dispersion, we firmly identified that the observed electric-dipole-active mode around 2.8 meV is magnetic in origin.

We further measured the T dependence of $\epsilon_1(\omega)$ and $\epsilon_2(\omega)$ in zero H to reveal the basic nature of this resonance, the results of which are displayed in Figs. 2(b) and 2(c), respectively. The conspicuous thermochromism is observed with the evolution of the conical-spin order below 50 K. The conical-spin state is characterized by the onset of spontane-

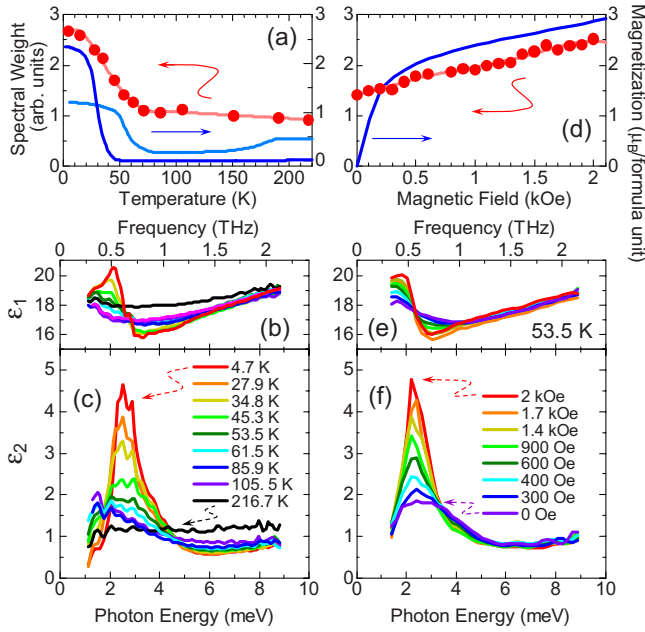


FIG. 2. (Color online) Gigantic thermochromism and magneto-chromism from electric-dipole-active magnetic resonances in $\text{Ba}_2\text{Mg}_2\text{Fe}_{12}\text{O}_{22}$. Temperature T dependence of the (b) real ϵ_1 and (c) imaginary ϵ_2 parts of the complex dielectric constant spectra $\epsilon(\omega)$ for $E^\omega \parallel [001]$ and $H^\omega \parallel [100]$ in the ferrimagnetic spin-collinear phase above 195 K, proper screw phase below 195 K, and conical phase below 50 K. (a) Spectral weight as a function of T (closed circles; the solid line is merely the guide to the eyes), as obtained by integrating the optical conductivity ($=\epsilon_0\omega\epsilon_2$, where ϵ_0 is the permittivity of vacuum) in the energy range of 2.0–3.9 meV. Magnetization M along $[001]$ is also shown (light solid line, M in 100 Oe; deep solid line, M in 0 Oe warming run after the field cooling of 50 kOe). Magnetic-field (H) dependence of (e) $\epsilon_1(\omega)$ and (f) $\epsilon_2(\omega)$, measured at 53.5 K. (d) Spectral weight (integrated in an energy range of 1.5–3.2 meV) as a function of H (closed circles; the solid line is merely the guide to the eyes). M along $[001]$ is shown by a solid line.

ous M along $[001]$; M measured in 0 Oe once after cooling to 5 K with applying H of 50 kOe is shown in Fig. 2(a). In the ferrimagnetic (collinear spin) phase above 195 K, the resonance feature is hardly discerned; but in the spin proper screw state below 195 K, $\epsilon_2(\omega)$ below 3 meV tends to grow in intensity with lowering temperature. Upon the proper screw to conical-spin transition around 50 K, the resonance becomes clearly discerned around 2.8 meV in $\epsilon(\omega)$. To see this tendency more clearly, we plot in Fig. 2(a) the spectral weight of the 2.8 meV peak as a function of T ; this unambiguously reveals the enhancement below ~ 70 K on cooling. The onset temperature (~ 70 K) is slightly higher than that of M , which arises perhaps from the fluctuation of the conical-spin order even above 50 K. We also plot M measured in 100 Oe [Fig. 2(a)], where temperature variation appears similar to that of the spectral weight below 70 K. These experimental results ensure the magnetic nature of the observed electric-dipole-active resonance with E^ω along $[001]$.

Since the observed resonance is enhanced with the development of the conical-spin order, we expect the change in this electric-dipole-active magnetic resonance intensity by

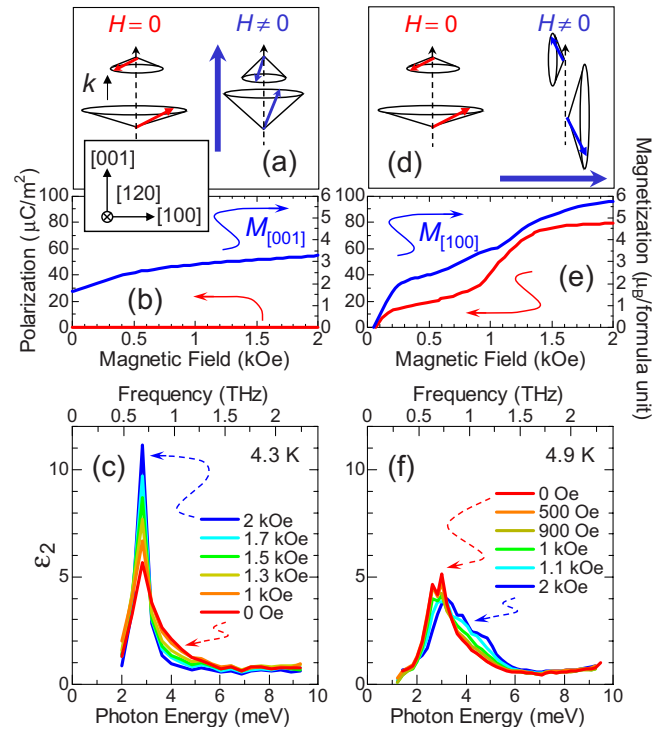


FIG. 3. (Color online) Electric-dipole-active magnetic resonances in magnetically induced longitudinal and transverse conical-spin phases of $\text{Ba}_2\text{Mg}_2\text{Fe}_{12}\text{O}_{22}$. Schematics of the (a) longitudinal and (d) transverse conical-spin structures, induced by external magnetic field H along $[001]$ and $[100]$, respectively. (a) In zero H , the cone axis is parallel to the propagation vector k along $[001]$. (d) On the contrary, the cone axis tilts toward $[100]$ when H is applied only along $[100]$, which produces the ferroelectric polarization P_s along $[120]$ shown in (e) (Ref. 20). Magnetization as a function of H along (b) $[001]$ and (e) $[100]$, measured at 5 K. Imaginary part of the complex dielectric constant spectra $\epsilon_2(\omega)$ for $E^\omega \parallel [001]$ and $H^\omega \parallel [100]$ as a function of H along (c) $[001]$ and (f) $[100]$, measured around 5 K. The specimens were polished to the thickness of 150–700 μm so as to gain the signal-to-noise ratio; the slight difference of the spectral shape shown in (c) and (f) comes from the restricted Fourier-transformed procedure due to the different sample thicknesses.

directly modifying the conical angle θ [Fig. 1(c)] through applying H along $[001]$. At 53.5 K [Fig. 2(d)] near the proper screw to conical-spin transition, H as low as 2 kOe can yield M as large as one third of the saturation magnetization M_s ($\sim 8\mu_B/\text{f.u.}$) and correspondingly increases θ from nearly zero to $\sim 20^\circ$ at 2 kOe, as derived by assuming that $\theta = \sin^{-1}(M/M_s)$. In fact, we found the conspicuous magneto-chromism at terahertz frequencies arising from a remarkable change in the electric-dipole-active magnetic resonance around this critical temperature [Figs. 2(e) and 2(f)] by an application of the external H . The spectral weight [Fig. 2(d)] increases by a factor of ~ 2 at 2 kOe. In accord with this, ϵ_1 around the resonance is strongly modified, for example, ϵ_1 below the resonant frequency is enhanced from 18 to 20. In a hitherto known multiferroic like TbMnO_3 ,⁷ the complete destruction of the spiral-spin structure by H on the order of several tesla is indispensable to yield such a large change in spectral weight as observed for $\text{Ba}_2\text{Mg}_2\text{Fe}_{12}\text{O}_{22}$.

To further reveal the particular role of the conical-spin structure in this resonance, we compare $\epsilon_2(\omega)$ in H applied along [001] [Fig. 3(c)] with that in H along [100] [Fig. 3(f)] at the lowest temperature (~ 5 K). In the latter case, P_s emerges along [120], perpendicular to the directions of k and H [Fig. 3(e)],²⁰ with developing the transverse conical-spin structure [Fig. 3(d)], whereas no P_s is generated [Fig. 3(b)] in the case for $H\parallel[001]$ [Fig. 3(a)]. The presence of such a conical-spin structure in H was recently confirmed by neutron scattering experiments,²⁹ being consistent with the behavior of P_s discussed in detail for $\text{Ba}_2(\text{Mg}_{1-x}\text{Zn}_x)_2\text{Fe}_{12}\text{O}_{22}$ with varying the magnetic anisotropy.³⁰ In contrast to the 5 K spectra for $H\parallel[001]$ in Fig. 3(c), which show the steep enhancement of the resonance as well as the case at 53.5 K [Fig. 2(f)], merely a tiny effect of H on the resonance is discerned in Fig. 3(f) for $H\parallel[100]$, apart from a slight accumulation of the spectral weight around 4.8 meV. Both longitudinal and transverse conical-spin structures can thus give rise to the similar electric-dipole-active magnetic resonance, irrespective of the presence or absence of P_s . Therefore, P_s , which is produced by the antisymmetric (Dzyaloshinskii-Moriya) interaction ($S_i \times S_j$),²⁷ is not responsible for the present electric dipole activity. The microscopic origin should be relevant to the local polarization produced by the underlying chemical lattice, which should be resonantly modulated by the exchange-striction ($S_i \cdot S_j$)-type spin-lattice

coupling.^{11,12} The spin-lattice coupling increases as the conical angle θ initially increases from zero [Fig. 3(c)], which may give rise to the effective coupling with E^ω along [001]. Therefore, the modification of θ can lead to gigantic thermochromism and magnetochromism as observed here.

In conclusion, based on the combined studies of terahertz time-domain spectroscopy and inelastic neutron scattering, we identified the sharp electric-dipole-active magnetic resonance at terahertz frequencies in the ordered conical-spin phase of $\text{Ba}_2\text{Mg}_2\text{Fe}_{12}\text{O}_{22}$. We also revealed the gigantic thermochromism and magnetochromism of this resonance as a result of the modification of the conical-spin angle by varying T and H . The present results may stimulate the investigations on a variety of noncollinear spin magnets to uncover the electric-dipole-active magnetic resonances. From a technological point of view, the observed gigantic magnetochromism yields a concept for future terahertz devices³¹ such as a tunable terahertz color filter controlled by H .

We thank S. Miyahara, N. Furukawa, H. Katsura, and N. Nagaosa for valuable discussions. This work was in part supported by Grant-In-Aids for Scientific Research (Grants No. 16076205 and No. 20340086) from the Ministry of Education, Culture, Sports, Science and Technology (MEXT), Japan. The neutron scattering experiment was performed under the User Program conducted by ISSP, University of Tokyo.

¹C. Kittel, *Introduction to Solid State Physics*, 7th ed. (John Wiley & Sons Inc., New York, 1996), Chaps. 15 and 16.

²V. G. Bar'yakhtar and I. E. Chupis, *Fiz. Tverd. Tela* (Leningrad) **11**, 3242 (1969) [*Sov. Phys. Solid State* **11**, 2628 (1970)].

³A. Pimenov, A. M. Shuvaev, A. A. Mukhin, and A. Loidl, *J. Phys.: Condens. Matter* **20**, 434209 (2008).

⁴N. Kida, Y. Takahashi, J. S. Lee, R. Shimano, Y. Yamasaki, Y. Kaneko, S. Miyahara, N. Furukawa, T. Arima, and Y. Tokura, *J. Opt. Soc. Am. B* **26**, A35 (2009).

⁵Y. Tokura, *Science* **312**, 1481 (2006).

⁶S.-W. Cheong and M. Mostovoy, *Nature Mater.* **6**, 13 (2007).

⁷A. Pimenov, A. A. Mukhin, V. Yu. Ivanov, V. D. Travkin, A. M. Balbashov, and A. Loidl, *Nat. Phys.* **2**, 97 (2006).

⁸H. Katsura, A. V. Balatsky, and N. Nagaosa, *Phys. Rev. Lett.* **98**, 027203 (2007).

⁹D. Senff, P. Link, K. Hradil, A. Hiess, L. P. Regnault, Y. Sidis, N. Aliouane, D. N. Argyriou, and M. Braden, *Phys. Rev. Lett.* **98**, 137206 (2007).

¹⁰N. Kida, Y. Ikebe, Y. Takahashi, J. P. He, Y. Kaneko, Y. Yamasaki, R. Shimano, T. Arima, N. Nagaosa, and Y. Tokura, *Phys. Rev. B* **78**, 104414 (2008).

¹¹R. Valdés Aguilar, M. Mostovoy, A. B. Sushkov, C. L. Zhang, Y. J. Choi, S.-W. Cheong, and H. D. Drew, *Phys. Rev. Lett.* **102**, 047203 (2009).

¹²S. Miyahara and N. Furukawa, arXiv:0811.4082 (unpublished).

¹³A. Pimenov, T. Rudolf, F. Mayr, A. Loidl, A. A. Mukhin, and A. M. Balbashov, *Phys. Rev. B* **74**, 100403(R) (2006).

¹⁴R. Valdés Aguilar, A. B. Sushkov, C. L. Zhang, Y. J. Choi, S.-W. Cheong, and H. D. Drew, *Phys. Rev. B* **76**, 060404(R) (2007).

¹⁵S. Pailhès, X. Fabrèges, L. P. Régnault, L. Pinsard-Godart, I. Mirebeau, F. Moussa, M. Hennion, and S. Petit, *Phys. Rev. B* **79**, 134409 (2009).

¹⁶M. Cazayous, Y. Gallais, A. Sacuto, R. de Sousa, D. Lebeugle, and D. Colson, *Phys. Rev. Lett.* **101**, 037601 (2008).

¹⁷M. K. Singh, R. S. Katiyar, and J. F. Scott, *J. Phys.: Condens. Matter* **20**, 252203 (2008).

¹⁸E. Golovenchits and V. Sanina, *J. Phys.: Condens. Matter* **16**, 4325 (2004).

¹⁹A. B. Sushkov, R. Valdés Aguilar, S. Park, S.-W. Cheong, and H. D. Drew, *Phys. Rev. Lett.* **98**, 027202 (2007).

²⁰S. Ishiwata, Y. Taguchi, H. Murakawa, Y. Onose, and Y. Tokura, *Science* **319**, 1643 (2008).

²¹K. Taniguchi, N. Abe, S. Ohtani, H. Umetsu, and T. Arima, *Appl. Phys. Express* **1**, 031301 (2008).

²²N. Momozawa, Y. Yamaguchi, and M. Mita, *J. Phys. Soc. Jpn.* **55**, 1350 (1986).

²³T. Kimura, G. Lawes, and A. P. Ramirez, *Phys. Rev. Lett.* **94**, 137201 (2005).

²⁴Y. Yamasaki, S. Miyasaka, Y. Kaneko, J.-P. He, T. Arima, and Y. Tokura, *Phys. Rev. Lett.* **96**, 207204 (2006).

²⁵H. Murakawa, Y. Onose, K. Ohgushi, S. Ishiwata, and Y. Tokura, *J. Phys. Soc. Jpn.* **77**, 043709 (2008).

²⁶N. Momozawa, Y. Nagao, S. Utsumi, M. Abe, and T. Yamaguchi, *J. Phys. Soc. Jpn.* **70**, 2724 (2001).

²⁷H. Katsura, N. Nagaosa, and A. V. Balatsky, *Phys. Rev. Lett.* **95**, 057205 (2005).

²⁸R. M. Nicklow, *J. Appl. Phys.* **42**, 1672 (1971).

²⁹S. Ishiwata *et al.* (unpublished); H. Sagayama, K. Taniguchi, N. Abe, T. Arima, Y. Nishikawa, S. Yano, Y. Kousaka, J. Akimitsu, M. Matsuura, and K. Hirota, *Phys. Rev. B* **80**, 180419(R) (2009).

³⁰S. Ishiwata, Y. Taguchi, Y. Tokunaga, H. Murakawa, Y. Onose, and Y. Tokura, *Phys. Rev. B* **79**, 180408(R) (2009).

³¹M. Tonouchi, *Nat. Photonics* **1**, 97 (2007).